Determining the accommodative response from wavefront aberrations

Janice Tarrant School of Optometry, University of California, Berkeley, CA, USA

Austin Roorda School of Optometry, University of California, Berkeley, CA, USA

Christine F. Wildsoet School of Optometry, University of California, Berkeley, CA, USA

The purpose of this study was to evaluate some of the methods used to calculate objective refractions from wavefront aberrations, to determine their applicability for accommodation research. A wavefront analyzer was used to measure the ocular aberrations of 13 emmetropes and 17 myopes at distance, and 4 near target vergences: 2, 3, 4, and 5 D. The accommodative response was calculated using the following techniques: least squares fitting (Zernike defocus), paraxial curvature matching (Seidel defocus), and 5 optical quality metrics (PFWc, PFSc, PFCc, NS, and VSMTF). We also evaluated a task-specific method of determining optimum focus that used a through-focus procedure to select the image that best optimized both contrast amplitude and gradient (CAG). Neither Zernike nor Seidel defocus appears to be the best method for determining the accommodative response from wavefront aberrations. When the eye has negative spherical aberration, Zernike defocus tends to underestimate, whereas Seidel defocus tends to overestimate the accommodative response. A better approach is to first determine the best image plane using a suitable optical quality metric and then calculate the accommodative error relative to this plane. Of the metrics evaluated, both NS and VSMTF were reasonable choices, with the CAG algorithm being a less preferred alternate.

Keywords: accommodation, aberrations, optical quality metrics, myopia

Citation: Tarrant, J., Roorda, A., & Wildsoet, C. F. (2010). Determining the accommodative response from wavefront aberrations. *Journal of Vision, 10*(5):4, 1–16, http://journalofvision.org/content/10/5/4, doi:10.1167/10.5.4.

Introduction

An extensive amount of research has been undertaken to determine the best method for calculating the ocular refractive error from wave aberration measurements. The gold standard for these techniques has been to find agreement with, or improve upon, in terms of accuracy and precision, the results from a subjective refraction. Curiously, an equivalent effort has not been expended on developing methods for determining the accommodative response from wavefront aberrations; instead it has been assumed that methods for calculating refractive error are also applicable to accommodation. Below we first review the methods proven successful in calculating objective refractions, as well as their limitations. Then we discuss their usage in and suitability for accommodation studies.

Initial attempts at predicting refractive errors used the Zernike coefficients from measured second-order aberrations expressed in power vector notation (Thibos, Hong, Bradley, & Cheng, 2002). Despite the fact that subjects wore prescription lenses that optimized their visual acuity during the measurements, residual defocus was evident in many of their aberration maps. This finding suggested that the method for judging best focus during a subjective refraction was not based on the criterion of minimizing the wavefront variance over the entire uniformly weighted pupil. Furthermore, the Zernike coefficients for this residual defocus varied systematically with the Zernike coefficients for spherical aberration in a way that maximized visual acuity. From these results, it was inferred that the subjective best focus occurred when the wavefront error was minimized over the largest possible area of the central pupil.

A number of alternative methods that take into account the effect of the eye's high-order aberrations (HOAs) have since been proposed to estimate refractive errors. Guirao and Williams (2003) calculated the combination of sphere and cylinder that optimized different image quality metrics. One class of metrics was based on the wave aberration defined in the pupil plane and another was based on the retinal image plane. The pupil plane metrics minimized either the wave aberration root mean square (RMS) or the sum of all the spherical and cylindrical components. Both pupil plane metrics predicted subjective refraction poorly, with large errors in spherical equivalent refractive error. The retinal image plane metrics optimized one of the following: the Strehl intensity ratio, the entropy and intensity variance of the point spread function (PSF),

doi: 10.1167/10.5.4 Received July 21, 2009; published May 6, 2010 ISSN 1534-7362

the volume under the modulation transfer function (MTF), or the volume under the contrast sensitivity function. All performed better than the pupil plane metrics, the differences between predicted and subjective refractions being considerably smaller.

Research into the effects of aberrations on visual performance has found important application in the development of methods for determining objective refractions from wavefront aberrations. Applegate, Marsack, Ramos, and Sarver (2003) showed that certain Zernike terms, for example spherical aberration and defocus, can interact to improve acuity despite an increase in total wavefront error. When combined in the correct proportions, spherical aberration and defocus decrease the wavefront error over the center of the pupil. In agreement with previous research (Thibos et al., 2002), better visual acuity is attained when the wave aberration is reasonably flat over a greater region in the pupil center.

Marsack, Thibos, and Applegate (2004) investigated the interaction of wave aberrations in terms of the correlation of 31 metrics of optical quality to high contrast visual acuity. The metrics were classified into 2 main types, pupil plane metrics, defined by qualities of the shape of the wave aberrations, and image plane metrics, based on either the PSF or the optical transfer function (OTF), with some of the latter including a neural weighting component. They identified 6 metrics that could account for 70% or more of the variance in visual acuity.

In a related study, Cheng, Bradley, and Thibos (2004) used the same 31 metrics of image quality to evaluate the impact of HOA on subjective refractions. To determine which metrics best predicted the subjective refraction, defocus and astigmatism levels that optimized each metric were compared with the corresponding metric values that produced the best visual acuity for degraded retinal images. They found that subjective judgment of best focus does not minimize the RMS wavefront error nor create paraxial focus but makes the retina conjugate to a plane between these two.

Chen, Singer, Guirao, Porter, and Williams (2005) used an adaptive optics system to manipulate the aberrations of the eye, by way of investigating the ability of different image quality metrics to predict measured subjective image quality. Their results confirmed that some Zernike modes, such as spherical aberration and defocus, interact strongly in determining subjective image quality. Their neural sharpness metric, which captures the effectiveness of a PSF in stimulating the neural portion of the visual system, best described subjective image sharpness.

In a comprehensive study of the ability of optical quality metrics to predict subjective refractions, all 31 metrics (Marsack et al., 2004) were evaluated using a large population of 200 eyes (Thibos, Hong, Bradley, & Applegate, 2004). These metrics were compared with 2 surface fitting methods, least squares fitting (Zernike defocus) and paraxial curvature matching (Seidel defocus), designed to find the nearest sphero-cylindrical approximation to the wave aberration map. Five of the optical quality metrics were classified as reasonably accurate and among the most precise; 3 were based on pupil plane metrics and 2 on image plane metrics. Zernike defocus proved to be one of the least accurate methods for determining the spherical equivalent refractive error. Seidel defocus was the most accurate, although it was significantly less precise than some of the optical quality metrics. It was suggested that Zernike defocus and Seidel defocus appear to locate the two ends of the eye's depth of focus (DOF), consequently the optimum focus should lie somewhere between these limits.

One problem with utilizing optical quality metrics to calculate objective refractions in a clinical setting is that they are computationally expensive, requiring an iterative process to find the optimal result. To address this issue, Iskander, Davis, Collins, and Franklin (2007) proposed the use of refractive and curvature Zernike power polynomials, which represent the wave aberration in terms of dioptric power calculated from closed-form expressions derived from the Zernike wavefront coefficients. The refractive Zernike power polynomials are based on an estimated focal length, and the curvature Zernike power polynomials are based on an estimated wavefront curvature. These 2 methods were compared with the more familiar least squares and paraxial curvature matching techniques, which are also pupil plane measures with closed-form solutions. Of these 4 methods, the refractive Zernike power polynomials yielded the best correlation between the objective and subjective sphero-cylindrical refractions. This method also achieved a marginally better correlation with subjective refraction compared to the performance of a number of image plane metrics that took into account pupil apodization and neural weighting (Iskander, Collins, Buehren, & Davis, 2008).

Understanding the influences of ocular aberrations on accommodative responses and subjective refraction represents similar problems although the former has received far less research attention. That aberrations change with accommodation is a complicating variable. For example, in a large study of young adults by Cheng, Barnett et al. (2004), the wave aberrations were found to vary with accommodation, with Zernike spherical aberration showing the greatest change, always in the negative direction and in proportion to the change in the accommodative response.

Of direct relevance to the current study, Hazel, Cox, and Strang (2003) investigated the relationship between accommodative accuracy and aberrations using an autorefractor to measure accommodation and a wavefront sensor to measure aberrations. The wavefront sensor data were used to determine the paraxial sphero-cylindrical correction, the sphero-cylindrical correction required to minimize the variance of the HOA, and the total sphero-cylindrical correction (paraxial + spherical aberration) for natural and 2.9-mm pupil sizes. For both emmetropic and myopic subjects, the paraxial sphero-cylindrical correction underestimated the accommodative error. The total sphero-cylindrical correction overestimated the accommodative error for both refractive error groups compared

with autorefractor readings when calculated with natural pupil sizes and underestimated it for the 2.9-mm pupil diameter. The authors attributed the discrepancies in accommodative errors measured with an autorefractor versus a wavefront sensor to the influence of HOA.

In another relevant study, Plainis, Ginis, and Pallikaris (2005) examined the correlation between accommodative errors and changes in ocular aberrations and retinal image quality during accommodation. Accommodative responses were calculated from the measured wavefront using 2 techniques: the equivalent quadratic of the wave aberration map using paraxial curvature matching and the power of a focusing lens needed to optimize retinal image quality as quantified by a weighted MTF metric. They found that spherical aberration was the main HOA that contributes to image quality changes during accommodation. Furthermore, with spherical aberration shifting from positive to negative values with increasing accommodation, the one-to-one stimulus–response relationship should not be considered ideal, instead a lag for near targets and a lead for far targets would be predicted.

In a later study, Buehren and Collins (2006) also found an association between accommodative error and spherical aberration under natural pupil conditions. The accommodative response was calculated from the Zernike defocus term for both 3-mm and natural pupil sizes and retinal image quality was quantified using the visual Strehl ratio of the OTF (VSOTF; Cheng, Bradley et al., 2004; Thibos et al., 2004). Because of the good correlation between the location of the peak of the VSOTF and accommodative errors, they concluded that these "errors" serve to optimize retinal image quality.

It is interesting that while the latter two studies (Buehren & Collins, 2006; Plainis et al., 2005) use completely different methods to calculate accommodative responses (Zernike defocus and paraxial curvature matching, respectively), both arrive at the same conclusion, that spherical aberration significantly influences accommodative errors. Which of these methods is the more appropriate for determining accommodative errors? Or is neither? The purpose of the current study was to evaluate some of the optical quality metrics (OQM) that have proven successful in determining objective refractions from wave aberrations, to determine their ability to calculate the accommodative response. We also propose an alternate method that may be better suited to quantifying the mechanism of selecting optimum focus utilized by the accommodation system.

Methods

Subjects

Thirty young adult subjects (mean age: 23.5 ± 2.9 years, range: 19 to 31 years) participated in the study; 13 were emmetropic (mean spherical equivalent refractive error (S_E): 0.21 ± 0.20 D, range: plano to +0.50 D) and 17 were myopic (mean S_E: −3.47 ± 1.47 D, range: −1.25 to −5.75 D). Astigmatism was limited to ≤1.00 D, and anisometropia to <2.00 D. All subjects had normal corrected visual acuity (20/20 or better) and no binocular vision anomalies. Prior to data collection, binocular accommodative amplitudes and facility were assessed to be within normal parameters based on age.

The study protocol conformed to the provisions of the Declaration of Helsinki and was approved by the University of California, Berkeley Institutional Review Board. Informed consent was obtained from the participants after the nature and possible complications of the study were explained in writing.

Data collection

A COAS wavefront analyzer (Abbott Medical Optics, Albuquerque, NM) was used to measure ocular aberrations at distance and 4 near target vergences: 2, 3, 4, and 5 D. Measurements were made of the dominant eye under monocular viewing conditions. All subjects wore single vision soft contact lenses to correct their ametropia. To control for any effect of the contact lenses on aberration measurements, the emmetropes were also fitted with contact lenses; those with plano prescriptions wore +0.25 D lenses as their distance prescription.

The near target was an external letter chart, viewed monocularly through a beam splitter, and positioned at the appropriate distance for each target vergence. It consisted of 4 lines, each made up of 5 high contrast letters, and decreasing in size, such that at each of the 4 near viewing distances, one line had an angular subtense of 12.5 min of arc. Subjects were instructed to look at the middle letter of the appropriate line of letters and to keep the letters as clear as possible. For each test condition, 20 data sets were obtained from approximately 2 s of continuous recordings. Measurements were taken in the dark, with a small LED providing the illumination for the near target.

Data analysis

The wavefront data were exported as the Zernike coefficients, up to sixth order, calculated for a wavelength of 550-nm and natural pupil sizes. Accommodative responses for each target vergence were calculated using 3 methods adapted from those used in determining objective refractions (Thibos et al., 2004), and another method developed specifically for this project. Two of these methods are closed-form solutions (least squares fitting and paraxial curvature matching) and the other two are iterative procedures.

The refractive state of the eye can be calculated directly from the measured wavefront using either of the closed-form solutions. For an accommodating eye, the refractive

state determined by these 2 metrics provides a measure of the accommodative response.

The wave aberration is the difference between the measured wavefront and the reference wavefront for the target vergence. For example, for the distance target the reference wavefront is a plane wave and for the near targets it is a spherical wavefront with a radius of curvature equal to the target distance. The accommodative error is the difference between the accommodative response and the stimulus vergence. Therefore because the accommodative response is determined from the measured wavefront, the wave aberration provides a measure of the accommodative error.

The accommodative error can be calculated directly from the wave aberration using either of the closed-form solutions, or it can be derived from the accommodative response determined by these 2 metrics by calculating the difference between the response and the stimulus vergence. The accommodative error can also be calculated from the wave aberration using the through-focus procedure described below, and the accommodative response can then be derived from the accommodative error.

Least squares fitting (Zernike defocus)

This is a surface fitting procedure designed to find the quadratic surface that best fits the wave aberration map by minimizing the sum of squared deviations between the two surfaces. It is given by the second-order Zernike coefficients and minimizes the RMS of the wave aberration:

$$M = \frac{c_2^0 4\sqrt{3}}{r^2}, \quad (1)$$

where c_2^0 is the second-order Zernike coefficient for defocus and r is the pupil radius.

Paraxial curvature matching (Seidel defocus)

This is another surface fitting procedure that matches the curvature of two surfaces at the pupil center. It is given by the Zernike expansion of the Seidel formula for defocus (truncated here at the fourth order):

$$M = \frac{c_2^0 4\sqrt{3} - c_4^0 12\sqrt{5}}{r^2}, \quad (2)$$

where c_2^0 is the second-order Zernike coefficient for defocus, c_4^0 is the fourth-order Zernike coefficient for spherical aberration, and r is the pupil radius.

Maximizing optical or visual quality

This procedure mathematically adds or subtracts specific amounts of a spherical wavefront (Zernike defocus) to the measured aberration map, which includes all aberrations from second to sixth order. Using a suitable metric of optical quality (OQM), the optimum power M needed to maximize optical quality for the accommodating eye was determined. The OQM we evaluated were 5 identified as reasonably accurate and among the most precise: PFWc, PFSc, PFCc, NS, and VSMTF (Thibos et al., 2004).

Brief descriptions of these OQMs are given in Table 1. The first 3 metrics quantify optical quality based on wavefront quality, in terms of the flatness of the aberration map, measured by RMS error, slope, or curvature. The last 2 metrics quantify the visual effectiveness of the retinal image, taking into account the Stiles–Crawford effect. NS uses retinal image quality for point objects, weighting the PSF with a spatial sensitivity function that represents the neural visual system. VSMTF uses retinal image quality for grating objects, weighting the MTF by the neural contrast sensitivity function (CSF). Programs for computing the metrics were written in Matlab (The Mathworks) and verified using known examples.

The wave aberration was calculated, then for each metric the through-focus analysis determined the amount of additional defocus required to maximize the metric over a nominal range of −0.5 to +0.6 D. This was accomplished by mathematically adding a spherical wavefront to the measured aberration map in 0.1-D increments, then computing the PSF, MTF, retinal image, and the corresponding OQM. The defocus level with the maximum metric value was defined as the plane of best focus and the accommodative error was defined as the additional defocus required to optimize the metric. An example of the through-focus analysis is shown in Figure 1 for one of our myopic subjects and the 5-D target vergence.

Data analyses with the pupil fraction metrics proved to be problematic in that, for some subjects and stimuli, the location of the best image plane was not well defined and the metric did not converge to an optimum value, i.e., all 12 defocus values in the through-focus sequence resulted

Acronym	Description
PFWc	Pupil fraction for wavefront when critical pupil is defined as the concentric area for RMS_w < criterion ($\lambda/4$)
PFSc	Pupil fraction for slope when critical pupil is defined as the concentric area for RMS_s < criterion (1 arcmin)
PFCc	Pupil fraction for curvature when critical pupil is defined as the concentric area for B_{ave} < criterion (0.25 D)
NS	Neural sharpness
VSMTF	Visual Strehl ratio for MTF

Table 1. Acronyms and descriptions for the optical quality metrics.

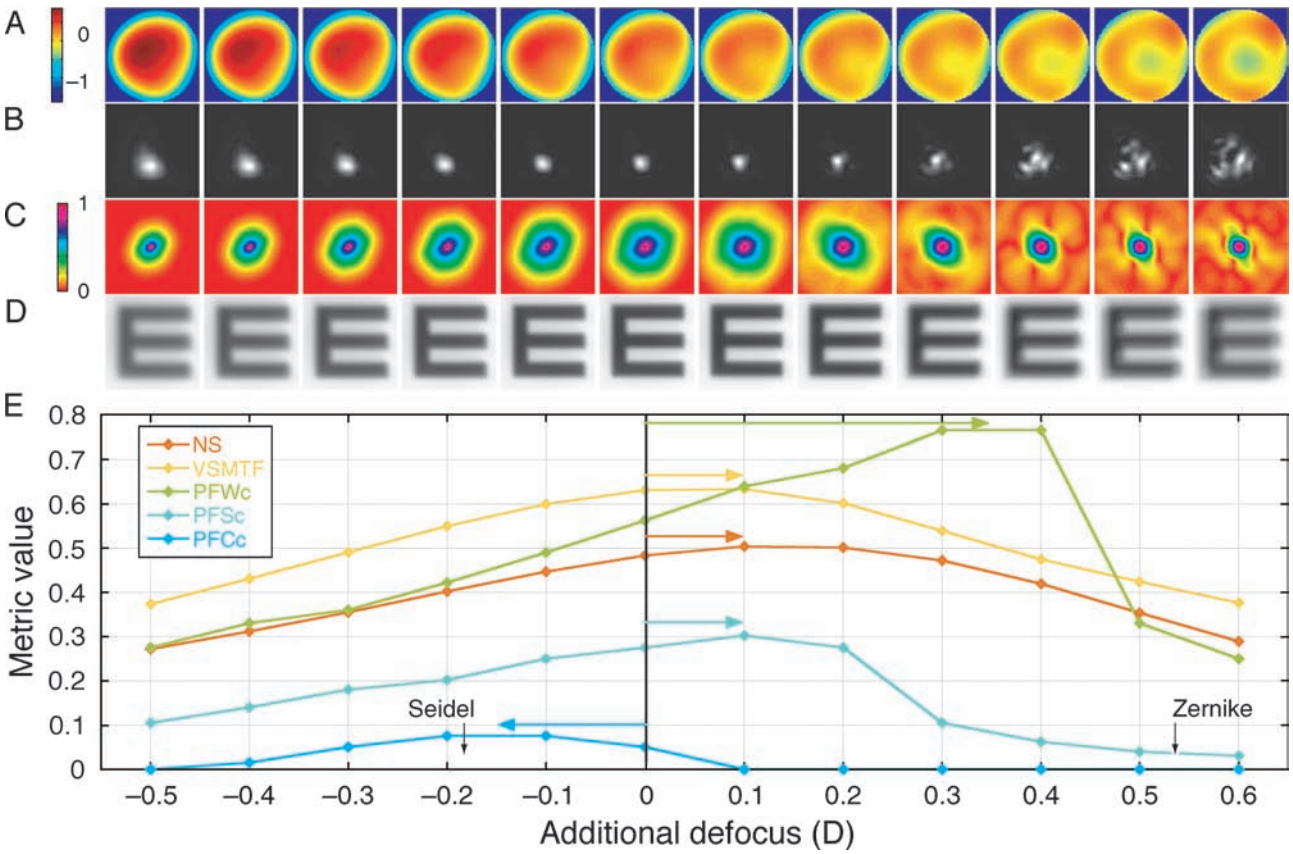

Figure 1. An example of the results from the through-focus analysis for a myopic subject and the 5-D target vergence. The image sequences are calculations of (A) the wave aberration contour map, (B) the PSF, (C) the MTF, (D) the retinal image of a 20/50 Snellen letter, and (E) the OQM values, adding defocus incrementally to the measured wave aberration. Colored arrows show the accommodative error determined by each metric. Metrics that peak to the right of the zero line indicate that additional defocus was needed to optimize image quality, corresponding to a lag of accommodation. Metrics that peak to the left of the zero line indicate a lead of accommodation. The black arrows show the accommodative errors calculated for Seidel defocus and Zernike defocus.

in the same value for the OQM. This problem was attributed to residual aberrations, such as astigmatism and spherical aberration, limiting the area over the center of the pupil where the wave aberration was sufficiently flat to meet the criterion specified for each metric. The PFSc metric proved to be the most robust of the 3 pupil fraction metrics and was considered a reasonable metric to use for calculating accommodative responses. The failure rate for the PFCc metric was very high, reaching 67% for the 4-D test condition and thus the results for this metric were not further analyzed. The performance of the PFWc metric, while better than that of the PFCc metric, was much poorer than that of the PFSc metric. Its results are presented later for interest; however, other metrics are considered better choices.

Contrast amplitude and gradient (CAG)

Because of the problems with the pupil fraction metrics just outlined, a new approach was developed based on the mechanism that the accommodative system appears to use to determine the appropriate response. This method takes into account studies of accommodation showing that the accommodative system optimizes contrast amplitude and gradient (Ciuffreda, 1999). The same sequence of 12 simulated retinal images, including an apodization function to take into account the Stiles–Crawford effect (Burns, Wu, Delori, & Elsner, 1995), was used to implement an algorithm that selected the image that best optimized both contrast amplitude and gradient. In addition, retinal images for a rotated E (90° counter-clockwise) were computed to more easily account for the biased effect of any residual astigmatism on image quality.

The intensity profile of the pixels from either the vertical or horizontal midline (vertical for the upright E and horizontal for the rotated E) of each image was used to quantify the contrast amplitude and gradient for that defocus level. A value of 0 corresponded to a black pixel and 1 corresponded to a white pixel. The location and values of the 2 maxima (2 white spaces between the "arms" of E) and 3 minima (the 3 "arms" of E) were found. A measure to quantify the contrast amplitude was calculated as the average of the difference between the values of the adjacent maxima and minima. A parabolic

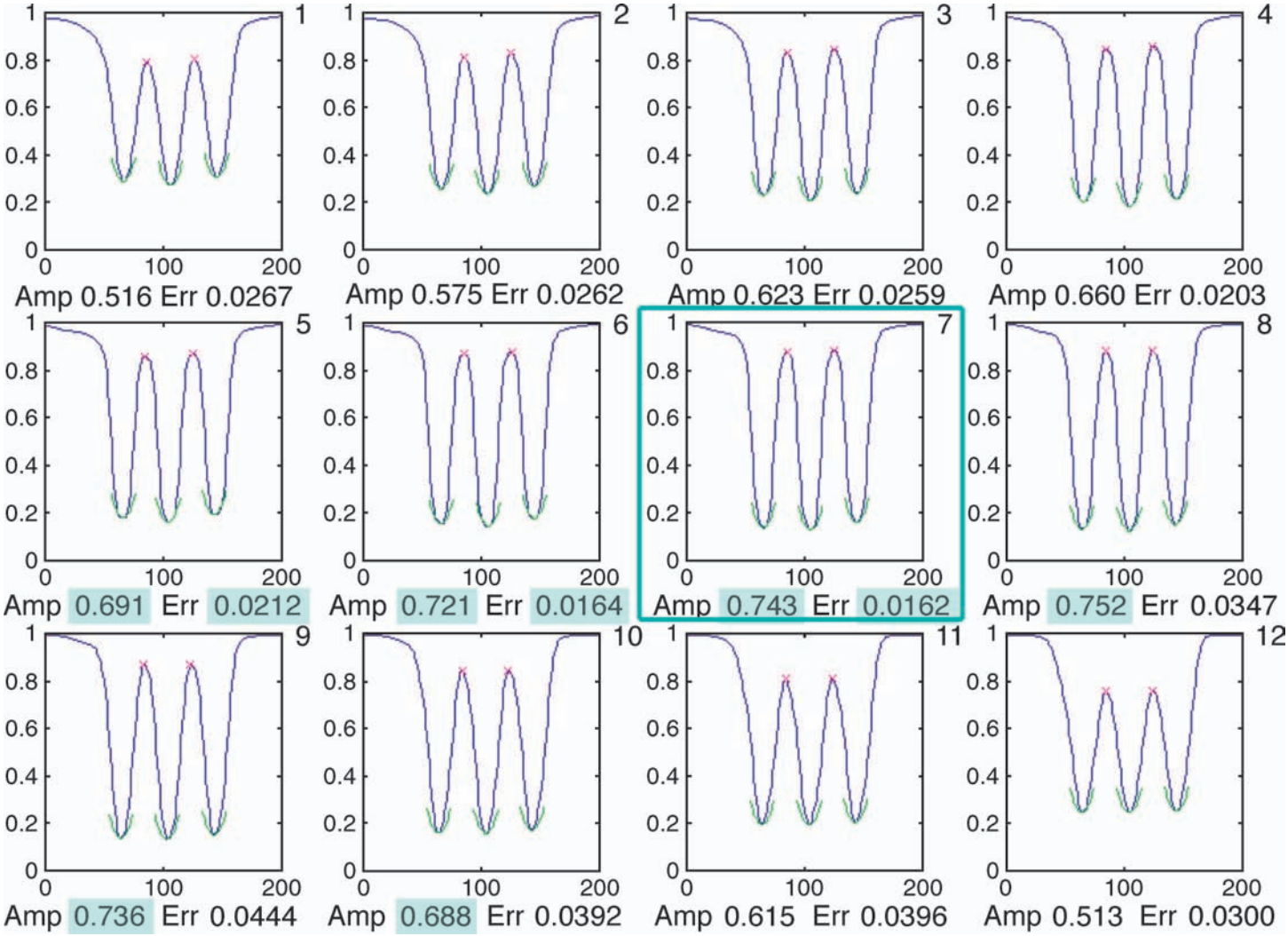

Figure 2. An example of the sequence of 12 intensity profiles for the upright E, used by the CAG algorithm. The green arcs show the parabolic functions fitted to the location of the 3 minima. The 6 images with the highest values for contrast amplitude (highlighted in green) were 5 to 10. The 3 images with the lowest RMS errors for the fitted parabola (highlighted in green), corresponding to the highest contrast gradients, were 5 to 7. Image 7 was chosen by the algorithm to best optimize both contrast amplitude and gradient (framed in green).

function was fitted to the location of the 3 minima and the RMS error for each was calculated to quantify the contrast gradient.

The 6 images with the highest values for contrast amplitude for the sequence of upright "E's" and the 6 highest for the rotated "E's" were identified. Only the images that were common to both sets of 6 were used in the next step. For this set of images, the 3 images with the highest values for contrast gradient (i.e., lowest error to the fitted function) for both the upright and rotated E's were selected. Two different methods were used to determine the "best" image from this subset. The first method gave each image a score of 10, 5, or 3, ranked from lowest error (best) to highest error (worst). The 2 scores for the upright and rotated E's were summed, with the best image having the highest score. The second method simply ranked the sum of the fitted errors for the upright and rotated E's, the best image having the lowest error sum.

This procedure for the upright E is depicted in Figure 2 for the same data shown in Figure 1. For both the upright and rotated E's, images 5 to 10 had the highest contrast amplitude. Of these, the 3 images with the "best" contrast gradients were 5 to 7 for the upright E, and 6 to 8 for the rotated E. Thus, image 7 scored 20, image 6 scored 8, image 8 scored 5, and image 5 scored 3, indicating that image 7 was the best for the first method (CAG1). The lowest combined error was also for image 7, identifying it as the best for the second method (CAG2).

Other aberrations

Astigmatism values were converted to diopters, using power vector notation, to allow comparisons of

measurements made with different natural pupil sizes (Thibos, Wheeler, & Horner, 1997):

$$J_0 = \frac{c_2^2 2\sqrt{6}}{r^2}, \quad (3)$$

$$J_{45} = \frac{c_2^{-2} 2\sqrt{6}}{r^2}, \quad (4)$$

where c_2^2 and c_2^{-2} are the second-order Zernike coefficients for astigmatism and r is the pupil radius.

Coma was converted to diopters using the equation for equivalent defocus (Thibos et al., 2002):

$$M_e = \frac{4\sqrt{3}\text{RMS error}}{r^2}, \quad (5)$$

where the RMS error is measured in microns and the pupil radius is in millimeters.

Excluded data

In subsequent analyses, 4 data sets were excluded: subject 6 (myope) at 2 D, subject 7 (emmetrope) at 2 D, and subject 14 (myope) at 4 and 5 D. In these cases, it was evident from the very reduced accommodative responses that the subjects were inattentive during the measurements. All excluded values were flagged as outliers in the statistical analysis.

Results

For both refractive error groups, there were leads of accommodation at distance for all metrics (Figure 3). For the emmetropes, there were lags of accommodation at all near targets for all metrics. For the myopes, however, there were lags of accommodation at all near targets only for Zernike defocus. With the OQMs, the myopes exhibited leads of accommodation for the 2- and 3-D targets, shifting to lags for the 4- and 5-D targets. While with Seidel defocus either no accommodative errors or small leads were seen at all near targets.

For both emmetropes and myopes, the dioptric separation in the accommodative responses calculated by the different metrics for each stimulus vergence appeared to be related to the level of spherical aberration. The spherical aberration shifted from positive to negative for the emmetropes between the 2- and 3-D stimuli (Figure 4), which corresponded to the smallest spread in the calculated

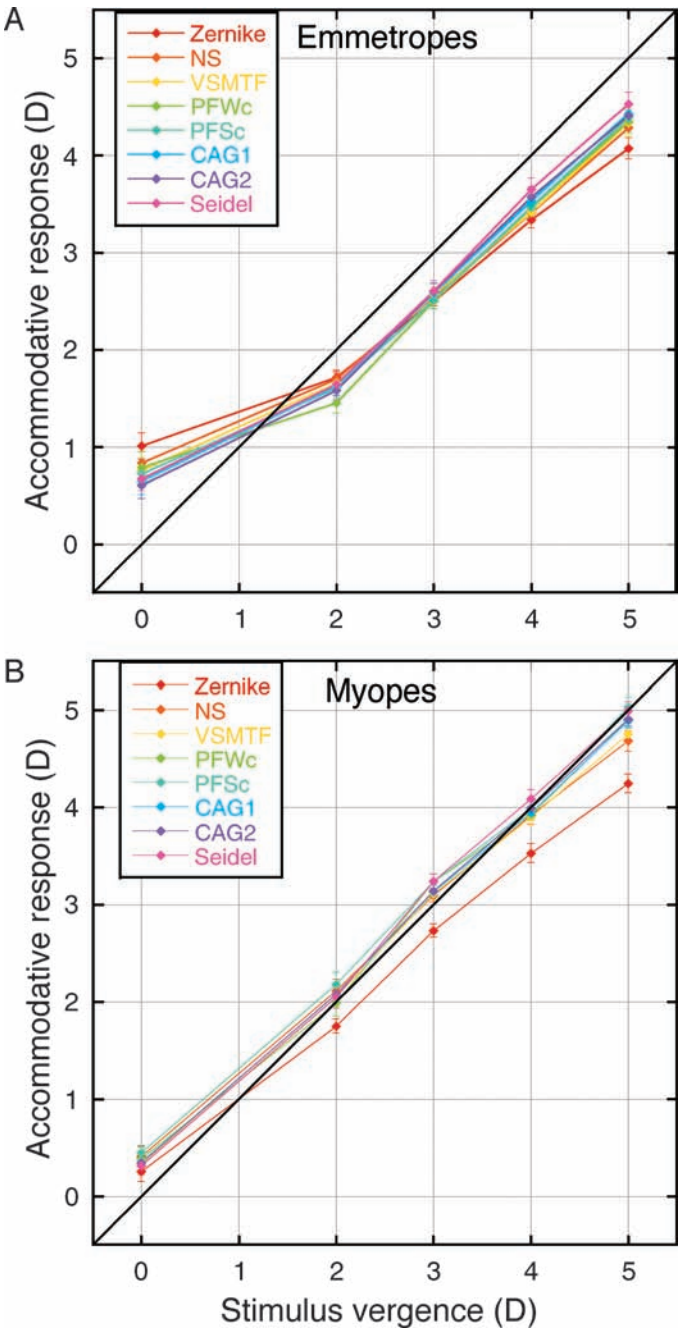

Figure 3. Accommodative responses calculated by each metric, for (A) emmetropes and (B) myopes. Error bars are ±*SEM*.

accommodative responses for the different metrics (Figure 3). For the myopes, spherical aberration was closest to zero with the distance target (Figure 4), which also corresponded to the smallest spread in calculated accommodative responses for the different metrics (Figure 3).

For each refractive error group, a one-way repeated-measures ANOVA was used to compare the differences between the accommodative responses calculated by each metric, for each stimulus level. For the emmetropes at the distance test condition, there was a significant difference

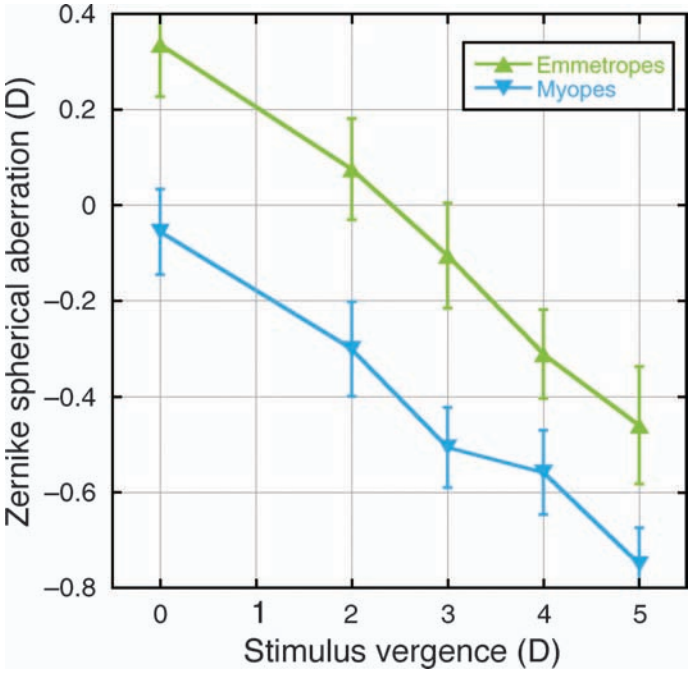

Figure 4. Zernike spherical aberration as a function of stimulus vergence for emmetropes and myopes. Differences between refractive error groups were significant ($p < 0.05$) for all stimuli except the 4-D vergence. Error bars are ±*SEM*.

in accommodative responses ($p < 0.001$) across metrics. An all-paired comparisons test, using the Tukey–Kramer method ($\alpha_{FW} = 0.05$), identified the results for Zernike defocus as significantly different from the results for Seidel defocus, PFSc, CAG1, and CAG2 for the distance target. At the 2-and 3-D stimuli, there were no significant differences in the values calculated by the different metrics. With the 4- and 5-D stimuli, there were significant differences in accommodative responses ($p < 0.001$) across metrics. The all-paired comparisons for the 4-D stimulus found the results for Zernike defocus to be significantly different to the results for Seidel defocus and CAG2, and the results for Seidel defocus also significantly different to the results for NS and VSMTF. The all-paired comparisons for the 5-D stimulus found the results for Zernike defocus to be significantly different to the results for Seidel defocus, PFSc, CAG1, and CAG2.

For the myopes at the distance test condition, there was no significant difference in the values calculated by the different metrics. With all near targets, there was a significant difference in accommodative responses ($p < 0.001$) across metrics. The all-paired comparisons, for all near vergences, found the results for Zernike defocus to be significantly different to the results for all other metrics. For the 5-D stimulus, there were also significant differences between the results for NS and the results for both Seidel defocus and PFSc, and between the results for VSMTF and the results for PFSc.

In comparing the difference in accommodative responses between emmetropes and myopes, only the metrics at the two extremes, Zernike defocus and Seidel defocus, were considered. Student's *t*-tests were used to compare the results for the two groups. For Zernike defocus, myopes had marginally higher accommodative responses than emmetropes, being significantly different only for the 3-D stimulus ($p < 0.05$). For Seidel defocus, myopes again recorded higher accommodative responses; here the differences reached statistical significance for all vergences ($p < 0.05$).

To better illustrate the differences between metrics, accommodative error is plotted in Figure 5. The sign convention adopted shows leads of accommodation as positive values and lags of accommodation as negative values. When ocular spherical aberration is negative, Seidel defocus and Zernike defocus appear to define the limits of the range of the accommodative error, with Seidel defocus always being higher by an amount equal to the magnitude of the spherical aberration in diopters (Equation 2). For both emmetropes and myopes, the trends for the accommodative errors calculated using the OQMs show NS and VSMTF nearer to Zernike defocus and CAG closer to Seidel defocus, with the pupil fraction metrics somewhere in the middle.

Linear regression analyses of the data shown in Figure 5, with accommodative error as the dependent variable and stimulus vergence as the independent variable, found the slopes to be significant for Zernike defocus, NS, and VSMTF, for both emmetropes and myopes. The slopes for CAG1 and CAG2 were also significant for the myopes. The flattest slope was observed for Seidel defocus for both refractive error groups. These data are summarized in Table 2, along with related correlation values.

The change in astigmatism and coma with accommodation was examined using Student's *t*-test. For both emmetropes and myopes, J_{45}, vertical coma, and horizontal coma were not significantly different from zero for any stimulus condition. This was also the case for J_0 for the emmetropes, except for the 2-D stimulus, where the average astigmatism increased slightly to 0.12 ± 0.03 D ($p < 0.005$). The myopes showed significant amounts of negative astigmatism (J_0) for all stimulus vergences, ranging from −0.14 ± 0.06 D to −0.21 ± 0.12 D ($p < 0.05$). This was not unexpected as the inclusion criterion for astigmatism allowed up to 1 D, which was not corrected by the spherical soft contact lenses.

In comparing the emmetropes with the myopes, there was no significant difference in J_{45} and vertical coma for any stimulus vergence. For the 3-D stimulus, there was a small, statistically significant difference in horizontal coma between emmetropes and myopes (0.07 ± 0.03 D, $p < 0.05$). For J_0, there was also a small but significant difference between the two refractive error groups at all stimulus vergences ranging from 0.18 ± 0.07 to 0.31 ± 0.08 D ($p < 0.05$).

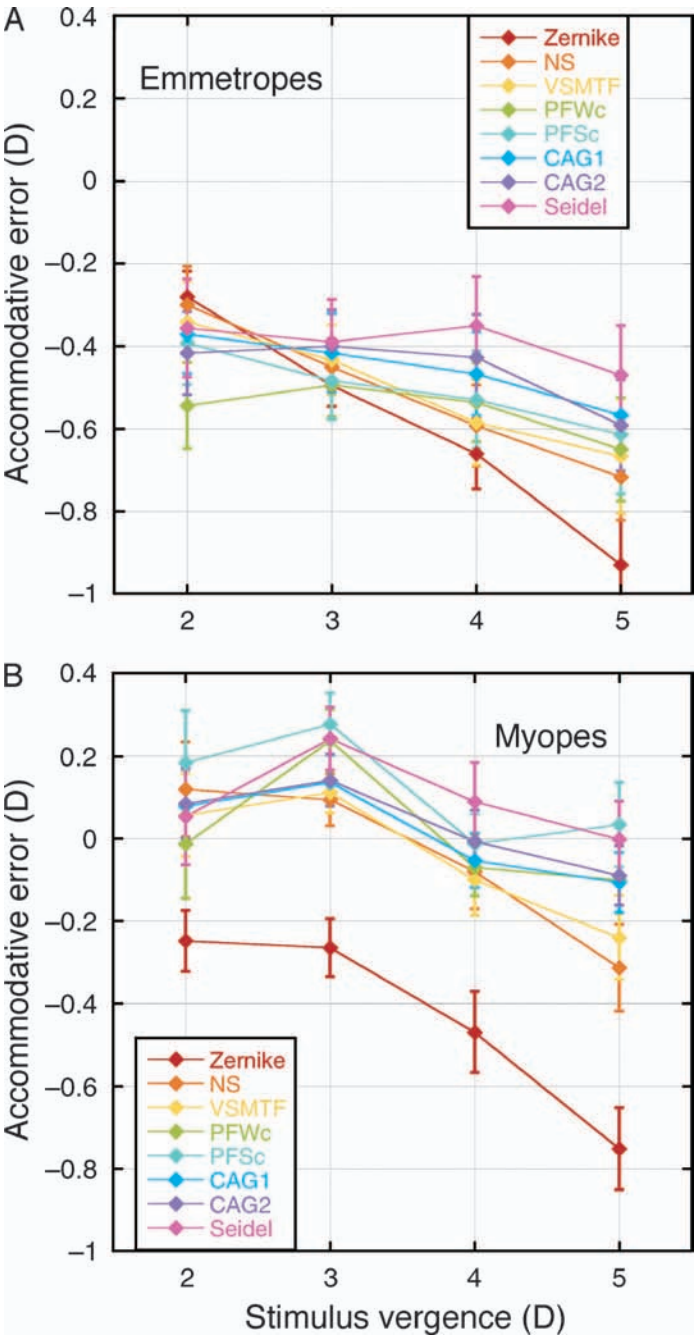

Figure 5. Accommodative errors determined by each metric, plotted as a function of stimulus vergence for (A) emmetropes and (B) myopes. Leads of accommodation are positive and lags are negative. Error bars are ±*SEM*.

Spherical aberration was converted to diopters using the second term of Equation 2. Values shifted from positive for emmetropes and approximately zero for myopes at distance to negative for both groups with increasing levels of accommodation (Figure 4). There was a significant difference in spherical aberration between emmetropes and myopes for all stimulus vergences except the 4-D stimulus ($p < 0.05$), with the myopes recording more negative values in all cases.

	Slope		Correlation	
Metric	Emmetropes	Myopes	Emmetropes	Myopes
Zernike	−0.211†	−0.171†	−0.657	−0.495
NS	−0.139†	−0.147†	−0.445	−0.406
VSMTF	−0.113†	−0.110†	−0.327	−0.341
PFWc	−0.038	−0.065	−0.135	−0.212
PFSc	−0.071	−0.076	−0.205	−0.218
CAG1	−0.064	−0.074†	−0.208	−0.277
CAG2	−0.055	−0.067†	−0.174	−0.250
Seidel	−0.030	−0.032	−0.085	−0.092

Table 2. Results of linear regression analyses for each metric, with accommodative error as the dependent variable and stimulus vergence as the independent variable. †Indicates slopes that are non-zero ($p < 0.05$).

The myopes tended to have smaller pupil sizes than the emmetropes, by approximately 0.5 mm (Figure 6). These differences were significant ($p < 0.05$) for the 2- and 3-D stimuli only.

The neural sharpness (NS) metric was used to estimate the depth of focus (DOF) from values calculated using the through-focus algorithm described in the Methods section over a range of ±1 D from the peak, in 0.1-D increments. These data points were fitted with a spline and the DOF was defined at the 80% level of the peak (Marcos, Moreno, & Navarro, 1999). The results (Table 3) indicate that the myopes had, on average, a slightly larger DOF. Student's *t*-test was used to compare the DOFs for the two refractive error groups, except for the 2-D stimulus where

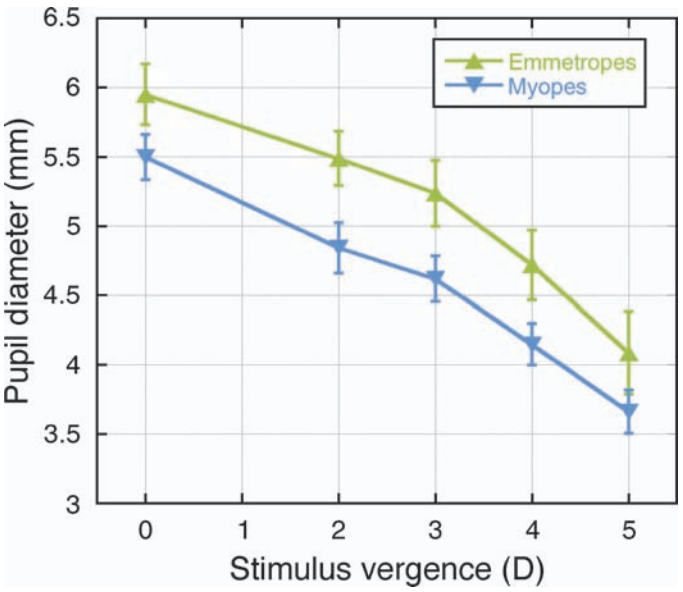

Figure 6. Pupil diameter plotted as a function of stimulus vergence for emmetropes and myopes. Differences between refractive error groups were significant for the 2- and 3-D stimuli only ($p < 0.05$). Error bars are ±*SEM*.

Stimulus vergence (D)	Depth of focus (D)	
	Emmetropes	Myopes
0	0.63 ± 0.07	0.74 ± 0.08
2	0.55 ± 0.04	0.89 ± 0.08†
3	0.61 ± 0.06	0.77 ± 0.06
4	0.56 ± 0.05	0.76 ± 0.05†
5	0.72 ± 0.05	0.87 ± 0.06

Table 3. Depth of focus (mean ± *SEM*) at each stimulus vergence for emmetropes and myopes. †Indicates significant differences between the two groups ($p < 0.05$).

the Aspin–Welch unequal variance test was used. Differences between the two groups were significant only for the 2-D and 4-D stimuli ($p < 0.05$).

Discussion

The main goal of our study was to identify an appropriate method for determining the accommodative response from wavefront aberrations. While it would be more expedient if one of the closed-form solutions, Zernike or Seidel defocus, were found to be suitable, it is not clear that either of these are the ideal method.

The accommodative responses calculated using Zernike defocus resemble data collected with an autorefractor (Tarrant, Severson, & Wildsoet, 2008). These results are also in agreement with those of other studies using wavefront sensors to measure accommodation (Buehren & Collins, 2006; Hazel et al., 2003). Identifying results that concur with optometer measurements, however, is not the primary goal, as readings from these instruments may also be affected by the presence of HOA (Campbell, Bobier, & Roorda, 1995; Collins, 2001). This leads to the question: what does the Zernike defocus tell us about the accommodative state of the eye?

Zernike defocus is the best fit sphere to the wave aberration and represents the average level of defocus (spherical power) across the pupil. (Note that although the Zernike polynomial for defocus is a parabolic function, over the dimensions of the pupil, the difference compared to a sphere is insignificant.) As the Zernike polynomials are orthogonal, Zernike defocus is independent of other aberrations, such as spherical aberration, astigmatism, coma, etc.; nevertheless, the retinal image quality is highly influenced by the interaction between certain aberrations.

The interaction of most interest for accommodation research is that between Zernike defocus and spherical aberration that has been examined in a number of visual performance studies (Applegate et al., 2003; Chen et al., 2005; Cheng, Bradley et al., 2004). These studies demonstrated that specific combinations of negative spherical aberration with negative defocus (hyperopic defocus) and positive spherical aberration with positive defocus (myopic defocus) produced images that were subjectively better focused than those with the same amounts of either spherical aberration or defocus alone. The implication of these results for accommodation is that an "ideal" one-to-one response on the accommodation stimulus–response curve measured with Zernike defocus is not ideal in terms of image quality. Instead, images will appear less blurred at distance with positive defocus to balance the positive spherical aberration present and at near with negative defocus to balance the negative spherical aberration resulting from accommodation. Plainis et al. (2005) and Buehren and Collins (2006) arrived at similar conclusions in their studies.

The effects of the interaction between Zernike defocus and spherical aberration on the wave aberration and retinal image quality are illustrated for positive spherical aberration and distance viewing in Figure 7, and for negative spherical aberration and the 5-D stimulus in Figure 8. The measured wave aberration and a simulation of the retinal image are in the center of these figures. To the left are simulations with negative defocus added in 0.25-D increments to the aberration map, and to the right are simulations adding positive defocus.

In Figure 7, when there is residual positive spherical aberration (leftmost image), this produces a flatter contrast gradient, creating blur in the edges of the letter E, despite more "accurate" accommodation (accommodative error: 0.14-D defocus). As positive defocus is added (to the right), the central region of the wave aberration flattens and image quality improves, despite a "worsening" accommodative error (0.64-D defocus). If too much defocus is added (continuing to the right past the measured values), there is an overall loss in contrast amplitude of the retinal image and a reduction in image quality.

In Figure 8, showing an accommodating eye, there is residual negative spherical aberration (rightmost image) and a poor contrast gradient, although only a negligible accommodative error (−0.04 D defocus). As negative defocus is added (to the left), the wave aberration flattens centrally and image quality improves, with a supposed increase in accommodative error (−0.54 D defocus). From these data, it is apparent that Zernike defocus is not a good measure, in terms of defining the plane of best focus, of accommodative error.

Does Seidel defocus provide a better option to Zernike defocus? Seidel defocus represents the curvature of the wavefront at the pupil center (Thibos et al., 2004). It is the paraxial power determined by rays traced through a small central region of the pupil, ignoring rays passing through the pupil periphery (Atchison, 2004). During "accurate" accommodation, the paraxial region of the measured wavefront should match the curvature of the vergence of the near target, thus the wave aberration would be flat at

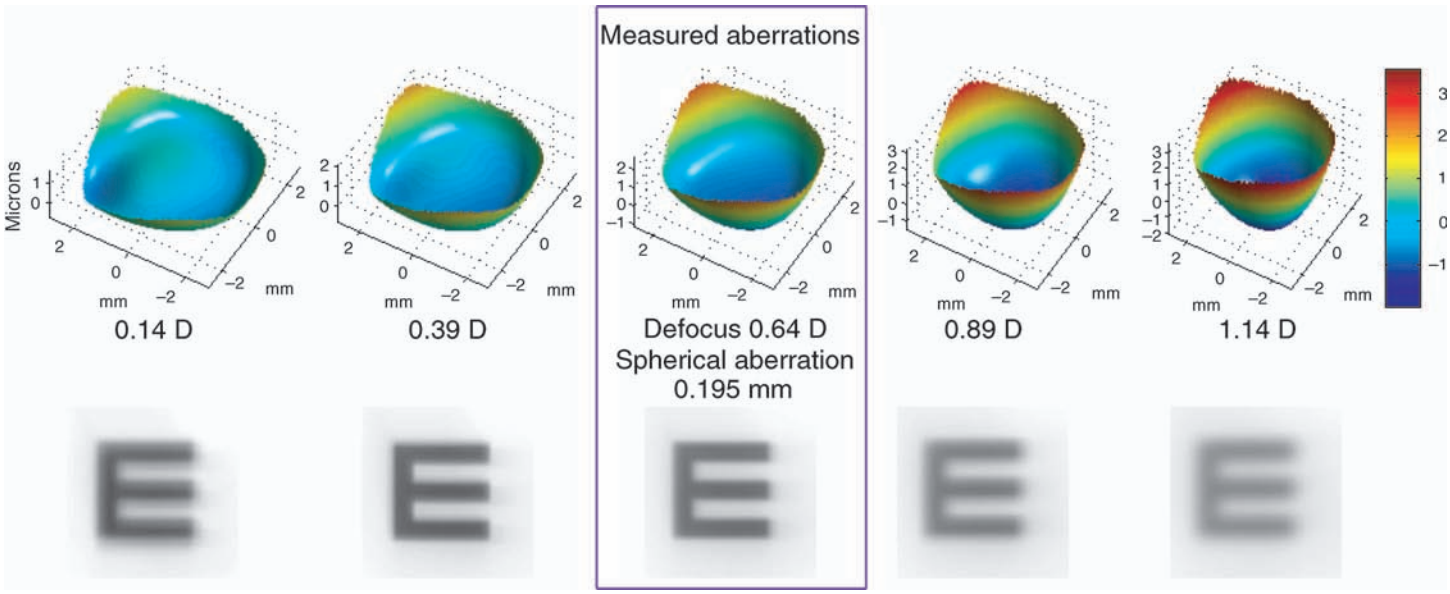

Figure 7. This through-focus analysis illustrates the interaction between Zernike spherical aberration and defocus for a myopic subject viewing the distance target. The measured aberrations are framed in violet; to the left are simulations adding negative defocus in 0.25-D increments to the wave aberration, and to the right are simulations adding positive defocus. Below each of the aberration map is a simulation of the retinal image for a 20/50 Snellen E.

the pupil center. The wave aberration maps in Figures 7 and 8 appear to meet this criterion. Seidel defocus was 0.0 D for the distance viewing condition (Figure 7) and 0.18 D for the 5-D stimulus (Figure 8).

From linear regression analyses, the slopes of the Seidel accommodative error were essentially zero for both refractive error groups, and there was no significant correlation between accommodative error and stimulus vergence. These results indicate that the accommodative error was approximately constant across all stimulus vergences, the average being 0.10 D for the myopes and −0.39 D for the emmetropes. Thus paraxial rays were focused quite accurately for the myopes, but not so for the emmetropes, who recorded significantly lower

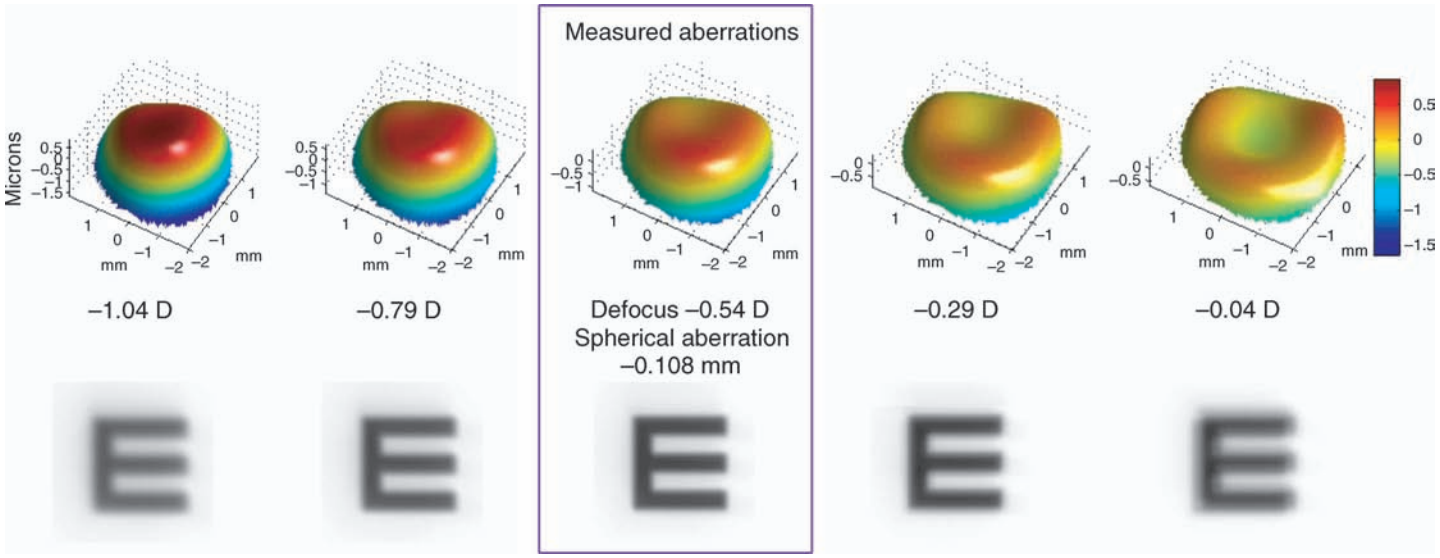

Figure 8. This through-focus analysis illustrates the interaction between Zernike spherical aberration and defocus for a myopic subject viewing the 5-D stimulus vergence. The measured aberrations are framed in violet; to the left are simulations adding negative defocus in 0.25-D increments to the wave aberration, and to the right are simulations adding positive defocus. Below each of the aberration map is a simulation of the retinal image for a 20/50 Snellen E.

accommodative responses compared to the myopes for all near target distances.

Two possible explanations are offered for the negative shift in Seidel accommodative error for the emmetropes compared to that of the myopes; either, it is only the Seidel error that is more negative, or the complete set of accommodative errors (Seidel + through-focus metrics + Zernike) are all shifted in the negative direction. For the Zernike response, based on the interaction between spherical aberration and defocus, a larger accommodative error would be expected for conditions where the spherical aberration is more negative. This is the situation for each refractive error group; as spherical aberration becomes more negative with increasing stimulus vergence, the Zernike accommodative error also becomes larger. The emmetropes, however, exhibited smaller amounts of negative spherical aberration for all near targets compared to the myopes (Figure 4); therefore, their Zernike responses should have been correspondingly higher. Nevertheless, there was no significant difference in Zernike defocus between emmetropes and myopes, except for the 2-D stimulus vergence, with the myopes' response being higher.

These results suggested that the set of accommodative errors for all metrics was shifted in the negative direction for the emmetropes. Therefore, we considered whether there were any optical explanations, such as differences in other aberrations, pupil sizes, DOF, etc., that could explain this offset. There was no significant difference in horizontal or vertical coma and oblique astigmatism (J_{45}) between emmetropes and myopes. The myopes had, on average, significantly larger amounts of astigmatism (J_0) compared to the emmetropes, although in magnitude this difference was very small. Myopes also had smaller pupil sizes (Figure 6) compared to emmetropes, significantly different for the 2- and 3-D stimulus conditions. Both of these findings imply that the myopes should have a larger DOF compared to the emmetropes, which was supported by the results of the DOF estimates from the neural sharpness metric (Table 3).

While the idea that differences in DOF could explain differences in accommodative accuracy seems reasonable, 3 recent adaptive optics (AO) studies of accommodation illustrate that the relationship between DOF and accommodation is not simple (Chen, Kruger, Hofer, Singer, & Williams, 2006; Chin, Hampson, & Mallen, 2009; Fernandez & Artal, 2005). One common premise investigated by these studies was that correcting HOA should decrease the DOF and therefore improve the accommodative accuracy. However, Fernandez and Artal (2005) found that correcting astigmatism, coma, and trefoil had no effect on the accommodative response amplitudes of their 2 subjects. Chen et al. (2006) investigated the effect of removing astigmatism and HOA with AO. Of the 4 subjects who were able to accommodate with HOA corrected, none showed a significant difference in response gain with corrected aberrations. Similar results were reported by Chin et al. (2009), specifically, correction of astigmatism and HOA did not significantly affect the accommodative response gain of their 4 subjects.

With no apparent optical reason to account for the negative shift in accommodative error found with the emmetropes, an alternative possibility may relate to the stability of our subjects' refractive error. Accommodative lag has been shown to be highly correlated with myopia progression for both myopes and non-myopes (Allen & O'Leary, 2006), with larger lags associated with the development of myopic shifts in refractive error. A plausible, albeit highly unlikely, scenario is that a large proportion of our emmetropes were undergoing myopic shifts in their refractive errors while an equivalent number of our myopes had stable refractive errors.

An interesting feature of the Seidel accommodative error data was that there was no increase in lag of accommodation with increasing stimulus vergence. Changes in accommodative error associated with changes in DOF have been well documented (Ciuffreda, 1999). An increase in lag would be expected with higher accommodative stimuli, due to the increase in DOF that results from pupillary miosis, image degradation with increasing negative spherical aberration, and a reduction in visual acuity (Heath, 1956; Tucker & Charman, 1975; Ward & Charman, 1985). The finding that paraxial focus predicts a fairly constant accommodative error was also reported by Hazel et al. (2003), although the data from Plainis et al. (2005) do not show the same effect. This departure from the classical stimulus–response curve as determined with Seidel defocus suggests that it also may not be a good measure of the true accommodative error.

Furthermore, in the presence of aberrations, the best image plane of an optical system is not necessarily the paraxial image plane (Welford, 1986). It is also important to keep in mind that determining the best image plane is not the same as choosing the best geometric focus (i.e., circle of least confusion). For an optical system with spherical aberration, the best geometric focus (described by ray tracing) is located 3/4 of the way between the paraxial and marginal foci, whereas including the effects of diffraction, the best focus (determined by the PSF) is halfway between the two. There is no evidence that the accommodative system chooses the best geometric focus, on the contrary it may choose the best diffraction focus or one closer to the paraxial focus (Mouroulis, 1999).

The idea that the eye alters its accommodative state to bring into focus the best image plane instead of the paraxial image plane has been proposed in previous studies (Cui, Campbell, Voisin, & Charman, 1993). It is also consistent with research determining objective refractions from wavefront aberrations (Cheng, Bradley et al., 2004; Guirao & Williams, 2003; Thibos et al., 2004), in which the optimum focus was found to lie somewhere between the paraxial focus (Seidel defocus) and the least squares solution (Zernike defocus). Therefore, metrics that

identify the best image plane, and define accommodative error relative to this plane rather than the paraxial plane, should provide a more valid measure of the true accommodative response.

This was the basis of the through-focus procedure, which attempts to determine the optimum spherical power needed to maximize the optical or visual quality of the eye. The biggest challenge with this technique was to find a suitable OQM that quantifies image quality using the same criteria as the accommodative system. Of the metrics evaluated, the pupil fraction metrics were unsuitable for reasons already outlined; however, both NS and VSMTF appear to be reasonable choices. NS captures the effectiveness of a PSF for stimulating the neural portion of the visual system (Chen et al., 2005). The VSMTF weights the MTF by the neural CSF, and thus the modulation near the peak of the CSF (e.g., 6 cpd) is weighted maximally (Thibos et al., 2004). The CAG algorithm that endeavors to optimize both contrast amplitude and gradient of the retinal image, to mimic the mechanism used by the accommodative system (Ciuffreda, 1999), also warrants further investigation.

The striking difference in the stimulus–response curves between the emmetropes and the myopes raises the question of which curve represents the "expected" response. Based on the typical appearance of this curve (Ciuffreda & Kenyon, 1983), it appears that the emmetropes are accommodating "as expected"; however, this may not be the case. The above discussion suggests that the myopes' accommodative response curve is what should be expected. If the best image plane lies somewhere between Seidel defocus and Zernike defocus, then during accommodation when the eye has negative spherical aberration, the former would overestimate and the latter would underestimate the accommodative response.

Another consideration is the introduction of a systematic bias in our data analyses due to the wavelength selected to calculate the accommodative responses from the wave aberration data. Our choice was an estimate of which wavelength would be best focused on the retina over the range of stimulus vergences presented based on published data. Millodot and Sivak (1973) found that with white light illumination, the wavelength focused on the retina changed from red for distant objects to blue for near objects, and to green for target vergences approximating the resting state of accommodation. Rather than complicating the analyses further by using a different reference wavelength for each stimulus vergence, we chose 550 nm based on experimental evidence that demonstrated that the response curves in white and green illumination are very similar (Charman & Tucker, 1978). In addition, 550 nm is midway between the peaks of the photopigment absorption spectra for the long wavelength sensitive cones (L-cones) and the middle wavelength sensitive cones (M-cones) at 565 nm and 535 nm, respectively.

The effect of changing the reference wavelength is illustrated in Figure 9 using the measured aberrations for

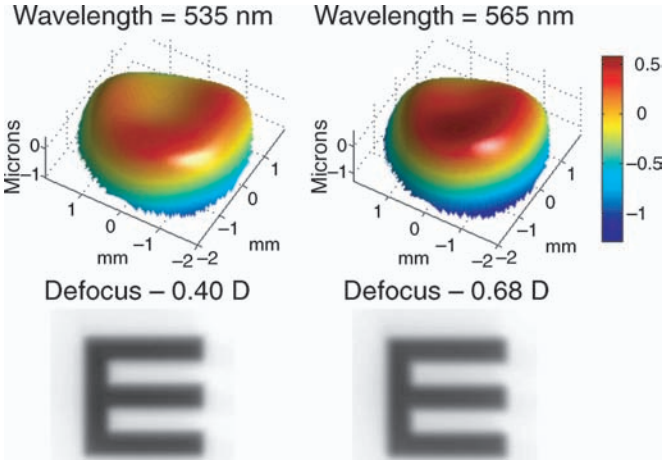

Figure 9. The effect of changing the reference wavelength; the wave aberration, Zernike defocus, and simulated retinal image for a myopic subject viewing the 5-D stimulus vergence, calculated for 535 nm (left images) and 565 nm (right images).

the same myopic subject and stimulus vergence (5 D) shown in Figure 8. When 550-nm light is in focus on the retina, the Zernike defocus is −0.54 D (Figure 8); however, for 535 nm this shifts to −0.40 D, and for 565 nm to −0.68 D (Figure 9) with the wave aberration becoming slightly more concave and convex, respectively.

The use of a single wavelength in our analyses also ignores an additional consequence of longitudinal chromatic aberration, that the 3 cone types effectively sample the retinal image in 3 different focal planes. Recent research supports the idea that the ratio of the L-cone contrast to the M-cone contrast influences the accommodative response (Rucker & Kruger, 2004a), with a further role for short wavelength sensitive cones (S-cones; Rucker & Kruger, 2004b). Based on the results from these studies, it was theorized that the habitual lag of accommodation may represent a balance between the S-cone contrast and the LM-cone contrast.

The implication of these results is that differences in accommodative responses between emmetropes and myopes could be associated with differences in sensitivities to L- and M-cone contrasts. One study reported an increased sensitivity to L-cone contrast relative to M-cone contrast with increasing myopia and a corresponding increase in mean accommodation level (Rucker & Kruger, 2006). While there appear to be no quantitative differences in chromatic aberration between emmetropes and myopes (Wildsoet, Atchison, & Collins, 1993), a shift in relative L:M-cone sensitivity could result from cone pigment polymorphism (Wagner-Schuman, Neitz, & Neitz, 2008) or differences in the relative numbers of L- and M-cones, perhaps accounting for differences between the emmetropic and myopic subjects reported here. However, it should be noted that all 3 chromatic aberration studies of accommodation did not consider monochromatic

aberrations. A model that considers both monochromatic and chromatic aberrations is likely to yield the most robust predictions.

Conclusions

When determining the accommodative response from wavefront aberrations, it appears that neither of the closed-form solutions, Zernike nor Seidel defocus, are the best method. When the eye has negative spherical aberration, which is typical during accommodation, Zernike defocus tends to underestimate the accommodative response, leading to the prediction of a larger lag of accommodation than is evident from the retinal image quality. Seidel defocus, on the other hand, tends to overestimate the accommodative response, resulting in either a smaller lag of accommodation, or even a lead of accommodation relative to the best image plane.

The data presented here suggest that a better approach to quantifying the accommodative response is to first determine the best image plane using a suitable OQM, and then calculate the accommodative error relative to this plane. Any metric chosen will provide a biased estimate of the best image plane depending on the specific feature of image quality optimized. Different metrics will therefore result in different values for the accommodative response; however, they should be in agreement to within a range comparable with the variability expected from the measurement and analysis procedures. Both NS and VSMTF meet these criteria and the CAG algorithm also shows promise.

In situations where a computational method requiring multiple iterations to determine the best image plane is not viable, a reasonable alternative could be simply to use the average of the Zernike defocus and Seidel defocus as a measure of the accommodative response. This would provide a numeric value similar to that obtained with one of the OQMs, however, without the insight gained from an analysis that also quantifies retinal image quality.

Acknowledgments

This research was supported by National Institutes of Health Grants K12 EY-017269 (J. T.) and EY-12392 (C. F. W.).

Commercial relationships: none.
Corresponding author: Janice Tarrant.
Email: jmtarrant@berkeley.edu.
Address: School of Optometry, University of California, Berkeley, 592 Minor Hall, CA 94720-2020, USA.

References

Allen, P. M., & O'Leary, D. J. (2006). Accommodation functions: Co-dependency and relationship to refractive error. *Vision Research, 46,* 491–505. [PubMed] [Article]

Applegate, R. A., Marsack, J. D., Ramos, R., & Sarver, E. J. (2003). Interaction between aberrations to improve or reduce visual performance. *Journal of Cataract and Refraction Surgery, 29,* 1487–1495. [PubMed] [Article]

Atchison, D. A. (2004). Recent advances in representation of monochromatic aberrations of human eyes. *Clinical and Experimental Optometry, 87,* 138–148. [PubMed] [Article]

Buehren, T., & Collins, M. J. (2006). Accommodation stimulus–response function and retinal image quality. *Vision Research, 46,* 1633–1645. [PubMed] [Article]

Burns, S. A., Wu, S., Delori, F., & Elsner, A. E. (1995). Direct measurement of human-cone-photoreceptor alignment. *Journal of the Optical Society of America A, Optics, Image Science, and Vision, 12,* 2329–2338. [PubMed] [Article]

Campbell, M. C., Bobier, W. R., & Roorda, A. (1995). Effect of monochromatic aberrations on photorefractive patterns. *Journal of the Optical Society of America A, Optics, Image Science, and Vision, 12,* 1637–1646. [PubMed] [Article]

Charman, W. N., & Tucker, J. (1978). Accommodation and color. *Journal of the Optical Society of America, 68,* 459–471. [PubMed] [Article]

Chen, L., Kruger, P. B., Hofer, H., Singer, B., & Williams, D. R. (2006). Accommodation with higher order monochromatic aberrations corrected with adaptive optics. *Journal of the Optical Society of America A, Optics, Image Science, and Vision, 23,* 1–8. [PubMed] [Article]

Chen, L., Singer, B., Guirao, A., Porter, J., & Williams, D. R. (2005). Image metrics for predicting subjective image quality. *Optometry and Vision Science, 82,* 358–369. [PubMed] [Article]

Cheng, H., Barnett, J. K., Vilupuru, A. S., Marsack, J. D., Kasthurirangan, S., Applegate, R. A., et al. (2004). A population study on changes in wave aberrations with accommodation. *Journal of Vision, 4*(4):3, 272–280, http://journalofvision.org/content/4/4/3, doi:10.1167/4.4.3. [PubMed] [Article]

Cheng, X., Bradley, A., & Thibos, L. N. (2004). Predicting subjective judgment of best focus with objective image quality metrics. *Journal of Vision, 4*(4):7, 310–321, http://journalofvision.org/content/4/4/7, doi:10.1167/4.4.7. [PubMed] [Article]

Chin, S. S., Hampson, K. M., & Mallen, E. A. (2009). Role of ocular aberrations in dynamic accommodation control. *Clinical and Experimental Optometry, 92,* 227–237. [PubMed] [Article]

Ciuffreda, K. J. (1999). Accommodation and its anomalies. In N. Charman (Ed.), *Visual optics and instrumentation* (pp. 231–279). Boca Raton, FL: CRC Press.

Ciuffreda, K. J., & Kenyon, R. V. (1983). Accommodative vergence and accommodation in normals, amblyopes and strabismics. In C. M. Schor & K. J. Ciuffreda (Eds.), *Vergence eye movements: Basic and clinical aspects* (pp. 101–173). Boston: Butterworth.

Collins, M. (2001). The effect of monochromatic aberrations on Autoref R-1 readings. *Ophthalmic and Physiological Optics, 21,* 217–227. [PubMed] [Article]

Cui, C., Campbell, M. C. W., Voisin, L., & Charman, W. N. (1993). Reducing aberration at the fovea by defocus. In *Ophthalmic and visual optics, technical digest series* (vol. 3, pp. 164–167). Washington, DC: Optical Society of America.

Fernandez, E. J., & Artal, P. (2005). Study on the effects of monochromatic aberrations in the accommodation response by using adaptive optics. *Journal of the Optical Society of America A, Optics, Image Science, and Vision, 22,* 1732–1738. [PubMed] [Article]

Guirao, A., & Williams, D. R. (2003). A method to predict refractive errors from wave aberration data. *Optometry and Vision Science, 80,* 36–42. [PubMed] [Article]

Hazel, C. A., Cox, M. J., & Strang, N. C. (2003). Wavefront aberration and its relationship to the accommodative stimulus–response function in myopic subjects. *Optometry and Vision Science, 80,* 151–158. [PubMed] [Article]

Heath, G. G. (1956). The influence of visual acuity on accommodative responses of the eye. *American Journal of Optometry and Archives of American Academy of Optometry, 33,* 513–524. [PubMed]

Iskander, D., Collins, M. J., Buehren, T., & Davis, B. (2008). The applicability of image quality metrics in the estimation of the sphero-cylindrical refraction from wavefront data of normal eyes. *Investigative Ophthalmology & Visual Science, 49,* E-Abstract 994. [Article]

Iskander, D. R., Davis, B. A., Collins, M. J., & Franklin, R. (2007). Objective refraction from monochromatic wavefront aberrations via Zernike power polynomials. *Ophthalmic & Physiological Optics, 27,* 245–255. [PubMed] [Article]

Marcos, S., Moreno, E., & Navarro, R. (1999). The depth-of-field of the human eye from objective and subjective measurements. *Vision Research, 39,* 2039–2049. [PubMed] [Article]

Marsack, J. D., Thibos, L. N., & Applegate, R. A. (2004). Metrics of optical quality derived from wave aberrations predict visual performance. *Journal of Vision, 4*(4):8, 322–328, http://journalofvision.org/content/4/4/8, doi:10.1167/4.4.8. [PubMed] [Article]

Millodot, M., & Sivak, J. (1973). Influence of accommodation on the chromatic aberration of the eye. *British Journal of Physiological Optics, 28,* 169–174. [PubMed]

Mouroulis, P. (1999). Aberration and image quality representation for visual optical systems. In P. Mouroulis (Ed.), *Visual instrumentation: Optical design and engineering principles* (pp. 27–68). New York: McGraw-Hill.

Plainis, S., Ginis, H. S., & Pallikaris, A. (2005). The effect of ocular aberrations on steady-state errors of accommodative response. *Journal of Vision, 5*(5):7, 466–477, http://journalofvision.org/content/5/5/7, doi:10.1167/5.5.7. [PubMed] [Article]

Rucker, F. J., & Kruger, P. B. (2004a). Accommodation responses to stimuli in cone contrast space. *Vision Research, 44,* 2931–2944. [PubMed] [Article]

Rucker, F. J., & Kruger, P. B. (2004b). The role of short-wavelength sensitive cones and chromatic aberration in the response to stationary and step accommodation stimuli. *Vision Research, 44,* 197–208. [PubMed] [Article]

Rucker, F. J., & Kruger, P. B. (2006). Cone contributions to signals for accommodation and the relationship to refractive error. *Vision Research, 46,* 3079–3089. [PubMed] [Article]

Tarrant, J., Severson, H., & Wildsoet, C. F. (2008). Accommodation in emmetropic and myopic young adults wearing bifocal soft contact lenses. *Ophthalmic and Physiological Optics, 28,* 62–72. [PubMed] [Article]

Thibos, L. N., Hong, X., Bradley, A., & Applegate, R. A. (2004). Accuracy and precision of objective refraction from wavefront aberrations. *Journal of Vision, 4*(4):9, 329–351, http://journalofvision.org/content/4/4/9, doi:10.1167/4.4.9. [PubMed] [Article]

Thibos, L. N., Hong, X., Bradley, A., & Cheng, X. (2002). Statistical variation of aberration structure and image quality in a normal population of healthy eyes. *Journal of the Optical Society of America A, Optics, Image Science, and Vision, 19,* 2329–2348. [PubMed] [Article]

Thibos, L. N., Wheeler, W., & Horner, D. (1997). Power vectors: An application of Fourier analysis to the

description and statistical analysis of refractive error. *Optometry and Vision Science, 74,* 367–375. [PubMed]

Tucker, J., & Charman, W. N. (1975). The depth-of-focus of the human eye for Snellen letters. *American Journal of Optometry and Physiological Optics, 52,* 3–21. [PubMed]

Wagner-Schuman, M., Neitz, M., & Neitz, J. (2008). Slowing the progression of myopia in children [Abstract]. *Journal of Vision, 8*(17):90, 90a, http://journalofvision.org/content/8/17/90, doi:10.1167/8.17.90.

Ward, P. A., & Charman, W. N. (1985). Effect of pupil size on steady state accommodation. *Vision Research, 25,* 1317–1326. [PubMed] [Article]

Welford, W. T. (1986). *Aberrations of optical systems*. Boston: Hilger, A.

Wildsoet, C. F., Atchison, D. A., & Collins, M. J. (1993). Longitudinal chromatic aberration as a function of refractive error. *Clinical and Experimental Optometry, 76,* 119–122. [Article]